QUANTITATIVE PREDICTIONS OF A NONCARRIER MODEL FOR GLUCOSE TRANSPORT ACROSS THE HUMAN RED CELL MEMBRANE

W. R. LIEB *and* W. D. STEIN

From the Polymer Department, The Weizmann Institute of Science, Rehovot, Israel. Dr. Lieb's and Dr. Stein's present address is the Institute of Life Sciences, The Hebrew University, Jerusalem, Israel.

ABSTRACT There is an increasing amount of experimental data on transport across biological membranes which cannot be readily accommodated by classical mobile carrier models. We propose models for membrane transport based upon current concepts in molecular enzymology, in which the membrane component involved in transport is an oligomeric protein which undergoes substrate-induced conformational changes. A number of paradoxical observations on glucose transport in the human erythrocyte are explained if the protein involved is a tetramer possessing two classes of binding sites with different affinities for glucose. We develop in detail a particular model of this type, the internal transfer model, in which transport occurs by transfer of substrate from one subunit to another of the protein. The fit of the predictions of the internal transfer model with most of the experimental data is very good. Those data which cannot be fitted by the model cannot be accounted for by any presently available model. We extend our model qualitatively to include the sodium-activated cotransport systems for sugars and amino acids.

INTRODUCTION

It has been obvious for a number of years that at the heart of the conventional analysis of the kinetics of sugar transport in the human erythrocyte lies a paradox. The kinetic parameters for sugar transport, K_m and V_{max}, have been determined by two standard experimental procedures. The one involves measurements with an asymmetric distribution of sugar (Sen and Widdas, 1962), the other with a symmetric distribution (Levine and Stein, 1966). Unexpectedly, these two procedures give widely divergent values for K_m and somewhat divergent values for V_{max}. When a conventional analysis fails to give a consistent explanation, it may be the conventions themselves which are at fault, suggesting the desirability of a qualitatively new approach. In this paper we present a new model for sugar transport based upon current concepts of molecular enzymology, a model which resolves this paradox.

We feel that the model can be extended to cover both further aspects of this present system and, in addition, many other membrane transport systems.

DESCRIPTION OF THE EXPERIMENTAL OBSERVATIONS

In the procedure introduced by Sen and Widdas (1962) (we will call this the Sen-Widdas procedure), cells are initially loaded with glucose to a concentration thought to be high enough to completely saturate the sugar efflux system. The loaded cells are then suspended in solutions of various glucose concentrations. That external concentration which reduces the net efflux to one-half the value found in the absence of external glucose ("V_{max}") is taken to be K_m . In the procedure employed by Levine and Stein (1966) (we will call this the equilibrium exchange procedure), cells are initially loaded with various concentrations of radioactively labeled glucose, then suspended in solutions of the identical concentration of nonradioactive glucose. The initial rate of loss of labeled glucose is determined. The data are plotted on a conventional double-reciprocal plot, from which the maximum rate of efflux (V_{max}) and that concentration of sugar which gives one-half this maximum rate (K_m) are determined.

When these two types of experiments were first performed (Sen and Widdas, 1962; Levine and Stein, 1966), the derived values of K_m and V_{max} were very different. This difference could have been due to the fact that the experiments had been performed in different laboratories by different investigators. Recently, however, in a responsible study, Miller (1968 *a*) has carried out both of these experiments and a number of others under strictly comparable conditions. Using the Sen-Widdas procedure, Miller (1968 *b*) found a K_m of 1.8 mM and a V_{max} of 104 mmoles/min per cell unit; using the equilibrium exchange procedure he found a K_m of 38 mM and a V_{max} of 260 mmoles/min per cell unit. (A cell unit is defined as a quantity of cells whose solvent water volume is 1 liter under isotonic conditions [Miller, 1968 *b*]. All experiments were performed at 20°C at pH 7.35.) Thus, the paradox remains.

PRELIMINARY CONSIDERATIONS FOR AN OLIGOMER MODEL

Although it is possible to modify the simple carrier model to account for these differences in V_{max} (e.g. by assuming that the rate of movement of a loaded carrier is faster than the rate of movement of an unloaded carrier [Levine and Stein, 1966]), to account also for the twentyfold discrepancy in the K_m values would require additional assumptions and additional arbitrary parameters. Rather than continuing to modify the conventional models, we have felt it to be of interest to consider models other than those of the mobile carrier type. In particular, the current emphasis in molecular biology upon the versatility of oligomeric proteins has led us to consider whether the paradox can be resolved by assuming that the transport system is an

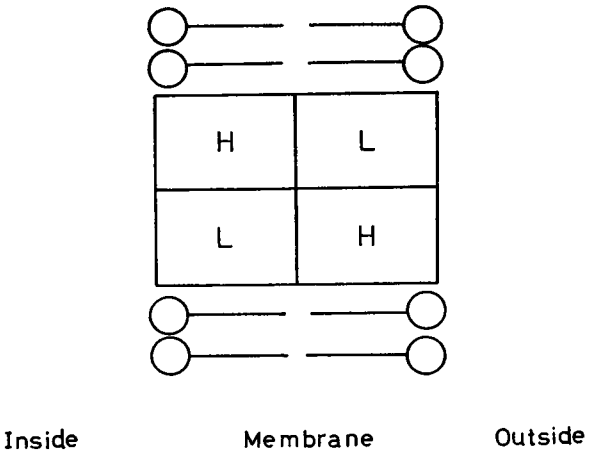

FIGURE 1 Schematic representation of a generalized tetramer model for membrane transport. H and L refer to protein subunits having different binding sites for substrate, the dissociation constants obeying the relationship $K_H \leqq K_L$. The terms "inside" and "outside" refer to the aqueous solutions bathing the cell interior and exterior, respectively. The tetramer is shown surrounded by lipid molecules.

oligomeric protein embedded in the membrane. We proceed to develop such a model and will show that the paradox is indeed resolved in a natural manner.

It is reasonable to assume from available data on the dimensions of proteins (Stryer, 1968) that such a molecule could extend through the cell membrane. Available data on turnover numbers for transport systems suggest that transport does not occur as a result of the diffusion of the protein as a whole (Stein, 1968). It is natural to assume that transport is the movement of substrate *within* such a protein, e.g., between subunits. The fact that two different K_m values appear in different experimental situations suggests that there exist two classes of binding sites for glucose, each binding site being represented by a different subunit of the oligomer. Such a model is depicted in Fig. 1. Here the transport system is a tetramer of the form H_2L_2, in which the H subunits bind glucose with a high affinity and the L subunits bind glucose with a low affinity. At this preliminary stage we do not wish to define in detail the molecular process of transport. We merely specify that in order for substrate to cross the membrane and emerge from the *trans* face of the transport system, it must first have been bound to a subunit at the *cis* face. The actual rate at which such a transfer occurs after binding to a given site will depend, we assume, upon the occupancy of the other three sites.

TRANSFER RULES FOR A SYMMETRIC TETRAMER MODEL

We show now how a consideration of the constraints imposed by the preceding experimental data allows us to develop the rules governing the behavior of such a

TABLE I

OCCUPANCY STATES OF TETRAMER FOR THE CASE OF ONLY ONE SUBSTRATE

Occupancy at *cis* face (H, L)	Occupancy at *trans* face (H, L)			
	(0, 0)	(1, 0)	(0, 1)	(1, 1)
(0, 0)	E(0, 0; 0, 0)	E(0, 0; 1, 0)	E(0, 0; 0, 1)	E(0, 0; 1, 1)
(1, 0)	E(1, 0; 0, 0)	E(1, 0; 1, 0)	E(1, 0; 0, 1)	E(1, 0; 1, 1)
(0, 1)	E(0, 1; 0, 0)	E(0, 1; 1, 0)	E(0, 1; 0, 1)	E(0, 1; 1, 1)
(1, 1)	E(1, 1; 0, 0)	E(1, 1; 1, 0)	E(1, 1; 0, 1)	E(1, 1; 1, 1)

A specific occupancy state of the tetramer is defined as a form of the tetramer which has substrate molecules bound to it at specific binding sites. The 16 possible occupancy states for a tetramer in contact with only one species of sugar are given in this table. The binding pattern at a given face (*cis* or *trans*) is denoted by (H, L), where H = 0 signifies no binding and H = 1 signifies binding at the H site, and L = 0 signifies no binding and L = 1 signifies binding at the L site. Notice that the semicolon as used here and throughout the paper is employed to separate the functional arguments concerning the *cis* face from those concerning the *trans* face.

tetramer. We consider at this stage the case of a single species of sugar. Since a given site may be either occupied or unoccupied, there are $2^4 = 16$ possible occupancy states of the protein. These are listed in Table I, where the notation used is explained. As an example, the occupancy state E(1, 0; 1, 1) refers to a tetramer having glucose bound at the *cis* H site and at both H and L *trans* sites. The problem is to determine the transfer rate constants corresponding to each of these 16 states. In general, there will be two transfer rate constants for each occupancy state — one for movement of substrate bound at the *cis* side into the *trans* solution, the other for movement of substrate bound at the *trans* side into the *cis* solution. If the system is symmetric for transport across the membrane, only 16 of these 32 rate constants are independent and need to be specified. (We consider the glucose transport system of the human erythrocyte to be symmetric, there being no evidence to the contrary.) It is sufficient to specify the 16 independent rate constants for transfer from the *cis* side to the *trans* solution. We adopt this procedure in the present paper. As an example, for the occupancy state E(1, 0; 1, 1) considered above, we have directly the transfer rate constant $k(1, 0; 1, 1)$ for *cis* to *trans* movement, while $k(1, 1; 1, 0)$ gives the transfer rate constant for *trans* to *cis* movement.

To illustrate how the experimental data constrain the possible range of transfer coefficients and, hence, the range of possible models for transport, we consider in detail the glucose transporting system of the human erythrocyte. The experimental data which we consider here are the results of the Sen-Widdas procedure and the equilibrium exchange procedure as performed by Miller (1968 *a*), discussed above. In the first place, consider the transfer rate constants for those tetramers which have

no substrate bound at the *cis* side. By definition, these tetramers cannot transport in the *cis* to *trans* direction. Therefore, $k(0, 0; 0, 0)$, $k(0, 0; 1, 0)$, $k(0, 0; 0, 1)$, and $k(0, 0; 1, 1)$ are equal to zero. We next consider the two occupancy states $E(1, 0; 0, 0)$ and $E(1, 0; 1, 0)$. We note that these tetramers, which have substrate bound only at the high affinity sites, are the prevalent forms at low substrate levels in an equilibrium exchange experiment. Yet the data of Miller (1968 *a*) for such an experiment show no deviation from a standard Michaelis-Menten relationship with a K_m of 38 mM, even at the lowest substrate concentrations used. Therefore, the contribution of these two occupancy states to the flux would seem to be insignificant, so that $k(1, 0; 0, 0)$ and $k(1, 0; 1, 0)$ are approximately equal to zero.

Let us next consider $E(1, 1; 1, 1)$, which is the dominant occupancy state in the equilibrium exchange experiment at limitingly high substrate concentration. Miller (1968 *b*) determined V_{max} = 260 mmoles/min per cell unit by a valid extrapolation to infinite substrate concentration. But $V_{max} = k(1, 1; 1, 1)T$, where T is the total amount of tetramer contained in a cell unit. Similarly, $E(1, 1; 0, 0)$ is the dominant occupancy state in an experiment in which the *trans* concentration of glucose is set at zero while the *cis* concentration approaches infinity. Miller (1968 *a*) measured the egress of glucose in a situation in which the external concentration was set at zero while the internal concentration was set at a concentration thought to be limitingly high. However, it can be shown from Appendix A that the operative K_m in such a situation is given by the K_S of the low affinity site (29 mM). When from this view the true V_{max} for egress is computed from Miller's data, V_{max} = 132 mmoles/min per cell unit. Here $V_{max} = k(1, 1; 0, 0)T$. It is therefore apparent that $k(1, 1; 1, 1) = 2[k(1, 1; 0, 0)]$.

Finally, we must consider $E(1, 0; 1, 1)$ and $E(1, 1; 1, 0)$. The relationship between the transfer rate constants for these occupancy states is revealed by a consideration of the Sen-Widdas procedure. Initially, when the external (*trans*) concentration of glucose is zero, the net flux is a maximum and is contributed mainly by $E(1, 1; 0, 0)$. When the external glucose concentration is set equal to the dissociation constant K_H of the high affinity site, $E(1, 1; 0, 0)$ is present at almost one-half of its initial value. However, to the extent that the K_m of the Sen-Widdas procedure is similar to K_H (which we show later), the net efflux at this latter concentration is also one-half of its initial value. Thus, $E(1, 1; 1, 0)$, the only other major occupancy state present at this glucose concentration, makes no contribution to the net flux; thus movement via this occupancy state in one direction must equal movement in the opposite direction. Therefore the transfer rate constant $k(1, 1; 1, 0)$ for *cis* to *trans* movement via the tetramer with this occupancy state can be equated to $k(1, 0; 1, 1)$, which gives the *trans* to *cis* rate constant for this occupancy state.

We emerge with the findings summarized in Table II. The dimensionless parameters x and y are the relevant transfer rate constants divided by the term f_1 (defined in the Symbols and Definitions). Notice that although for a given value of f_1T the value of the parameter y is completely determined by these experimental

TABLE II

CONSTRAINTS PLACED ON GLUCOSE TRANSFER RATE CONSTANTS BY EXPERIMENTAL DATA

Occupancy at *cis* face (H, L)	Occupancy at *trans* face (H, L)			
	(0, 0)	(1, 0)	(0, 1)	(1, 1)
(0, 0)	0	0	0	0
(1, 0)	0	0	—	x
(0, 1)	—	—	—	—
(1, 1)	y	x	—	$2y$

This table lists approximate values of the transfer rate constants divided by f_i for the occupancy states of Table I, using (as described in the text) experimental data for the human erythrocyte glucose transport system at 20°C, pH 7.35. A solid line indicates that the experimental data give no constraints for the specified transfer rate constants. For a given value of f_iT the value of y is completely determined by the available experimental data, whereas the value of x is undefined.

data, the value of x is undefined. It is important to emphasize that many members of the set of tetramer models satisfying the constraints of Table II will resolve the paradox of the divergent K_m and V_{max} values given by the Sen-Widdas and the equilibrium exchange procedures.

A SPECIFIC TETRAMER MODEL FOR THE GLUCOSE TRANSPORT SYSTEM

To choose from among the members of the set of models which satisfy the constraints of Table II, we must abstract a subset which conforms to additional experimental data and is also reasonable at a molecular level. We have had some success in doing this. We have chosen a model (Fig. 2), which although admittedly incomplete, is yet simple enough to be easily comprehended and analyzed in a quantitative manner. In this model, the internal transfer model, the tetrameric transport protein can exist in two conformation states (Fig. 3). In state A the four binding sites are exposed to the bathing solutions; in state B each pair of sites are separately in communication with one another across an internal pool. The transport process consists of the following steps: (*a*) substrate in the external solutions equilibrates with the binding sites of the protein in state A; (*b*) bound substrate allows the conformational change to state B; (*c*) within each pool the substrate redistributes itself, obligatorily binding to one or the other site according to the affinities of the binding sites (as we develop later); (*d*) internally bound substrate allows the conformation change back to state A; (*e*) substrate is released into the external solutions and the cycle begins again at step (*a*). As an example, the above cycle is illustrated in Fig. 3 for the occupancy state E(1, 0; 1, 1) which we have considered previously. Fig. 4

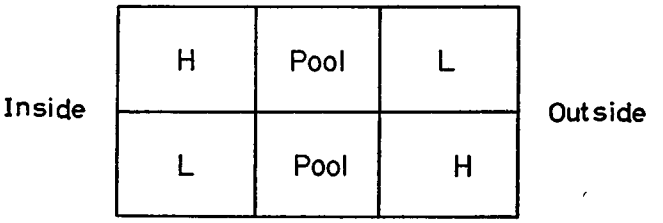

FIGURE 2 Schematic representation of the internal transfer model for membrane transport. This model, a specific member of the class represented by Fig. 1, is described in detail in the text.

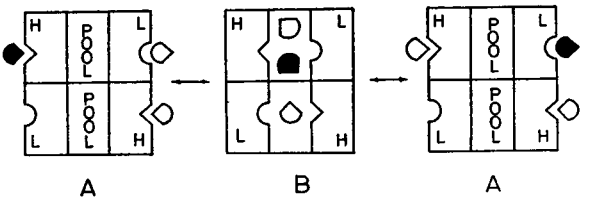

FIGURE 3 Illustration of the details of a transport event on the internal transfer model of Fig. 2. See text for explanation. The case considered is where $K_H \ll K_L$. Substrate initially bound at the left-hand (*cis*) side of the membrane is shaded. Notice that in the example chosen, the transformation from state B back to state A can, with equal probability, result in the substrate being redistributed as at the extreme left (no transport) or as at the extreme right (two molecules exchanged).

illustrates feasible semimolecular representations of the model based upon current concepts of molecular enzymology.

We depend heavily upon the concepts of Koshland (e.g. Koshland and Neet, 1968) in that we assume that the transition between the two conformational states A and B has a mandatory requirement for substrate. Such a requirement provides the specificity and absence of leak needed for efficient cell function. Although it is in general permissible for the system to possess different binding affinities for substrate in the two conformations (Monod, Wyman, and Changeux, 1965), we have not found it necessary to make this assumption for the glucose transport system of the human erythrocyte. It should be emphasized that in the transport event, it is primarily the rate of transition between conformational states that is the matter of most concern, not the equilibrium proportion of these two states. This contrasts with the situation for those proteins concerned primarily with ligand binding or subject to regulatory control. Note that Fig. 4 demonstrates that the separation of the two pools, as required by our model, may be only functional and not structural.

We now proceed to develop in detail the internal transfer model of Fig. 2. We shall consider the more general case of two substrates, e.g. glucose and sorbose, being transported simultaneously. Since a given site may be unoccupied, occupied by substrate 1, or occupied by substrate 2, there are $3^4 = 81$ possible occupancy

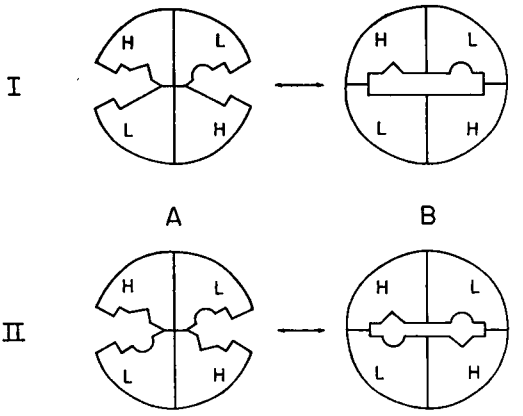

FIGURE 4 Semimolecular representations of the conformational states assumed by the transport system on the internal transfer model. Two possibilities (I and II) are considered. In I, a section through one channel of the tetramer is represented. A second, symmetrically disposed channel, lies in a parallel section. In II, a section through the single channel of the tetramer is shown. If this latter representation is to be valid, the binding site(s) on the sugar must be so located that, once in the internal pool, steric constraints determine that a given sugar can bind to only the upper or the lower pair of receptors on the tetramer.

states of the protein. Our problem now is to determine the transfer rate constants corresponding to each of these 81 states. Of the independent transfer constants, 16 refer to states previously considered in Table I. We will show later that the present model is consistent with the constraints listed in Table II.

Consider an occupancy state $E(i, j; i', j')$, where the indices i, j, i', j' can have any of the values 0, 1, or 2. The values 1 and 2 refer to occupancy by substrates 1 and 2, respectively. Otherwise the conventions are as given under Table I. In the model of Fig. 2 the transfer rate constant ${}^1k(i, j; i', j')$ for movement of substrate 1 in the *cis* to *trans* direction is given by

$$ {}^1k(i, j; i', j') = f(i, j; i', j')[{}^1p_H(i; j') + {}^1p_L(j; i')]. \quad (1) $$

(A similar equation holds for substrate 2 with the superscript 2 replacing superscript 1.) In equation 1 the term $f(i, j; i', j')$ is the transition frequency, the number of transitions per minute from state A to state B and back again to state A; the terms ${}^1p_H(i; j')$ and ${}^1p_L(j; i')$ are the probabilities that molecules of substrate 1 bound on the *cis* face at sites H and L, respectively, will be transferred to the opposite site and, hence, to the *trans* solution.

We first take up the problem of the transition frequency. We assume that between states A and B there exists an activation energy barrier. The probability of surmounting this barrier in the absence of bound substrate is assumed to be negligible. However, the presence of bound substrate at any given site lowers the activation barrier sufficiently to allow occasional transitions to occur. To the extent that the

contribution of each bound site is independent, the transition frequency is simply proportional to the number of sites occupied. Thus,

$$f(i, j; i', j') = Nf_1, \tag{2}$$

where f_1 is the transition frequency when only one site is occupied, and N is the total number of occupied sites, given by the number of nonzero terms among the indices i, j, i', j'. Other choices of activation rules are possible and give comparable predictions. The present set has been chosen for its simplicity and symmetry.

We next consider the rules for the redistribution of substrate within the pools. Notice that each pool contains one high affinity H site and one low affinity L site and that a pool may contain zero, one, or two substrate molecules only. At first sight, it might appear that the desired rules are entirely arbitrary. However, as we show in Appendix B, the requirement that no part of the system be capable of developing a concentration gradient of either substrate between the external solutions (given no energy input) leads to a unique solution. The results of the analysis are given in Appendix B.

It may be useful to comment upon these results. Notice that when only one sugar enters a given pool, it will, with a high probability, leave the pool via the high affinity H site, regardless of which site it entered upon (e.g. see equations B 12 and B 13 with ${}^1K_H \ll {}^1K_L$). Thus, in the example of Fig. 3, sugar enters the lower channel via the *trans* H site and in most cases leaves the pool in the same manner, thus

TABLE III

GLUCOSE TRANSFER RATE CONSTANTS AS PREDICTED BY INTERNAL TRANSFER MODEL

Occupancy at *cis* face (H, L)	Occupancy at *trans* face (H, L)			
	(0, 0)	(1, 0)	(0, 1)	(1, 1)
(0, 0)	0	0	0	0
(1, 0)	$\frac{K_H}{K_H + K_L}$	$\frac{2K_H}{K_H + K_L}$	1	$\frac{3}{2}$
(0, 1)	$\frac{K_L}{K_H + K_L}$	1	$\frac{2K_L}{K_H + K_L}$	$\frac{3}{2}$
(1, 1)	2	$3\left(\frac{1}{2} + \frac{K_H}{K_H + K_L}\right)$	$3\left(\frac{1}{2} + \frac{K_L}{K_H + K_L}\right)$	4

This table lists the predictions of the internal transfer model with independent activation via any site. The tabulated values are those of the transfer rate constants (divided by f_1) as given by equations (A 2), (A 3), (B 17), and (B 18) in the Appendexes. Notice that at 20°C, when K_H = 1.35 mM and K_L = 29 mM (Appendix A), these values approximate closely the corresponding values specified by the experimental constraints in Table II.

making no contribution to any measurable flux. A significant contribution will arise in a one-substrate situation only when this substrate enters on a low affinity L site. When two identical sugars enter a given pool, they have an equal probability of emerging at either site (see equation B 14). Finally, when two different sugars enter a given pool, the situation is more complex, with the exit probabilities being given by equations B 15 and B 16.

Now that all of the terms on the right-hand side of equation 1 are calculable, we can obtain all of the transfer rate constants. In particular, we are now in a position to check that our model satisfies the constraints of Table II. Thus, we have calculated the relevant transfer rate constants using equations 1 and 2 and Appendix B; the results are listed in Table III. Notice that, as required, the terms in Table III approach the values of the corresponding terms in the matrix of constraints (Table II) as the ratio of the dissociation constants K_H:K_L tends to zero. (As will be shown shortly, the experimental data at 20°C are fitted best by K_H = 1.35 mM and K_L = 29 mM, giving a value of 0.04 for the term $K_H/[K_H + K_L]$ in Table III.) Thus, the present model satisfies the constraints of Table II, and is thus a member of the set of models which resolve the paradox revealed by the Sen-Widdas and equilibrium exchange procedures.

DETAILED PREDICTIONS OF THE TETRAMERIC INTERNAL TRANSFER MODEL

With the transport rate constants established, it is a simple but tedious matter to calculate the predictions of the model for any experimental situation. The procedure for doing this is given in Appendix A. In this section we compare the predictions of the model with representative experimental data obtained by Miller (1968 *a*). All of these data were obtained under comparable experimental conditions at 20°C and pH 7.35.

We consider first the two experiments which showed up clearly the problem to which we have addressed ourselves. The predicted and experimental data are shown for the equilibrium exchange experiment (Fig. 5) and for the Sen-Widdas experiment (Fig. 6). It is clear that the internal transfer model gives a very satisfactory fit to the experimental data over the range of glucose concentrations used. Notice that in order to obtain these theoretical predictions only three parameters (K_H , K_L , f_1T) had to be assigned.

It is generally assumed that sorbose shares with glucose the same transport system in the human erythrocyte. On the simple carrier model the two sugars would compete for the common binding site. Thus, it would be expected that glucose would inhibit the movement of sorbose with an inhibition constant K_I equal to the dissociation constant K_S of the glucose-carrier complex (Stein, 1967). On the internal transfer model the situation is more complex. Although glucose will still compete with sorbose for access to the transport system, those molecules of sorbose

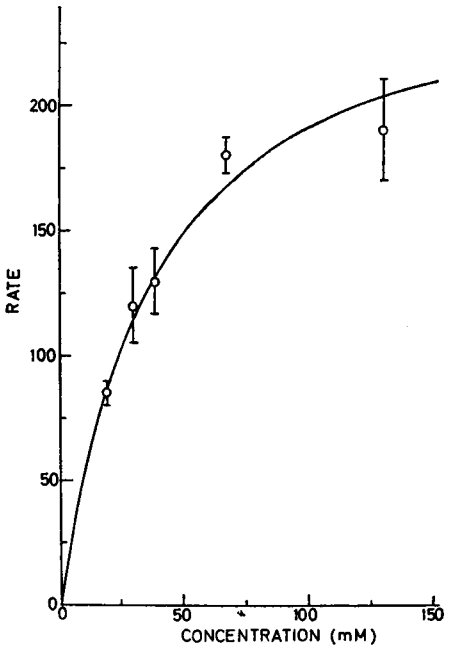

FIGURE 5 Equilibrium exchange procedure. The initial rate of loss of radioactive glucose (mmoles/min per cell unit) is plotted against the equilibrium concentration of glucose. The means (±SD) of the experimental points are taken from Table IV of Miller (1968 *a*). The solid line is the prediction of the internal transfer model for K_H = 1.35 mM, K_L = 29.0 mM, and f_iT = 65 mmoles/min per cell unit.

which do gain access will be transported at a greater than normal rate as a result of glucose binding at other sites. Thus, the operative K_I will not be equal to either of the dissociation constants for glucose. The predicted and experimental data for the inhibition of both sorbose entry and exit by varying concentrations of glucose present at both sides of the membrane are shown in Fig. 7. The accord of theory with experiment is again very satisfactory. Notice that the operative K_I derived from Fig. 7 is about 12–14 mM, intermediate between the values of K_H and K_L for glucose.

We have thus been able to explain, on the basis of the internal transfer model, the first three type of experiments performed by Miller (1968 *a*). It remains for us to consider his remaining two procedures, which have only recently been applied to the human erythrocyte glucose transport system. We proceed to discuss these procedures. We will show that although we do not find quantitative agreement with experiment, inherent complications in these types of experiment raise the possibility that they do not present a valid test of any transport model.

The first of these procedures involves measuring the amount of labeled glucose in cells at various times after these cells, initially loaded with a high concentration of unlabeled glucose, are placed in a very large volume of solution containing radioactive glucose at a low concentration. It is found that the concentration of labeled glucose in the cells transiently, but substantially, exceeds the concentration in the external solution. Transport of a molecular species against its electrochemical potential in such circumstances is known as countertransport. Countertransport

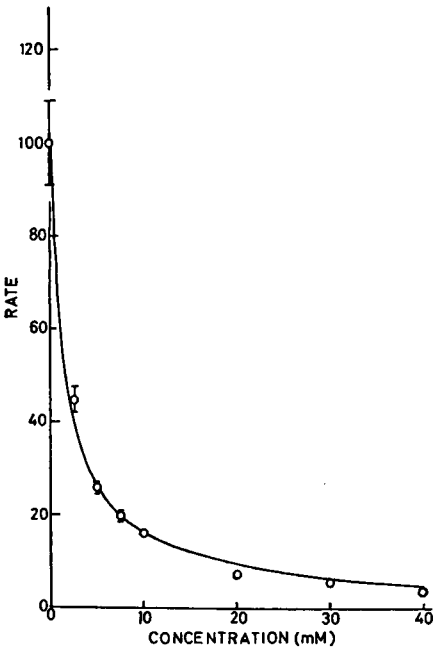

FIGURE 6 Sen-Widdas procedure. The initial rate of loss of glucose (mmoles/min per cell unit) from cells previously equilibrated with a 130 mM glucose solution and then suspended in a solution with the concentration given on the abscissa is shown. The means (±SD) of the experimental points are taken from Table I of Miller (1968 *a*). The solid line is the prediction of the internal transfer model for K_H = 1.35 mM, K_L = 29.0 mM, and f_iT = 65 mmoles/min per cell unit.

is commonly thought to require the existence of a mobile carrier (Wilbrandt and Rosenberg, 1961), although the contrary has been ably argued by Vidaver (1966). In Fig. 8 we demonstrate that the internal transfer model, which would not be generally considered to be a mobile carrier model (in the sense that a given binding site is not on our model alternately exposed to the *cis* and *trans* bathing solutions), does indeed predict countertransport. However, the accord of the quantitative predictions of the internal transfer model (Fig. 8, curve *b*) with the experimental data (Fig. 8, curve *c*) of Miller (1968 *a*) is not good. We must consider the possible reasons for this lack of agreement.

Curve *a* of Fig. 8 gives the prediction of the internal transfer model for the total cellular concentration of glucose, labeled and unlabeled, as a function of time. Unfortunately, the experimental counterpart of this curve is not presented by Miller. However, the initial slope of curve *a* agrees with the results in Fig. 2 of his paper (Miller, 1968 *b*); and, where experimental data are available (Harris, 1964; Sen and Widdas, 1962), the general shape of curve *a* is confirmed. Thus, it is reasonable to assume that curve *a* gives a good approximation to the true situation, independent of the choice of model. From curves *a* and *c* it is possible to make a revealing analysis. If it is assumed that the interior of the erythrocyte behaves as a well-mixed compartment under the conditions of the experiment, it is possible to compute the value of the undirectional influx of glucose at any time. The procedure is given in Appendix C, with the results shown in the insert to Fig. 8. Notice that this analysis

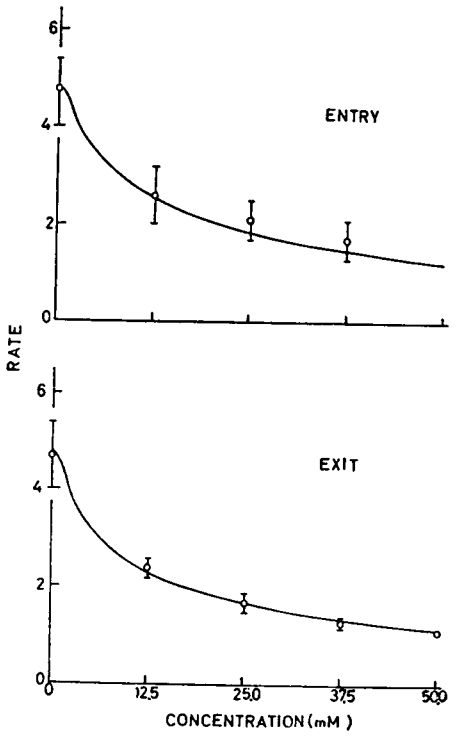

FIGURE 7 Inhibition of sorbose transport by glucose. The initial rate of transport of sorbose (mmoles/min per cell unit) is plotted against the concentration of glucose with which the cells were previously equilibrated. In the entry experiment (upper curve), a solution of sorbose was added to the equilibrated cell suspension to give a final concentration of 230 mM. In the exit experiment (lower curve), the cells were first equilibrated with 230 mM sorbose and then with 230 mM sorbose plus the glucose. Finally, the cells were resuspended in 230 mM sucrose (to prevent swelling) plus the glucose. The means (±SD) of the experimental points are taken from Table II of Miller (1968 *a*). The solid lines are the predictions of the internal transfer model for: ${}^1K_H$ = 1.35 mM, ${}^1K_L$ = 29.0 mM for glucose; ${}^2K_H$ = 1500 mM, ${}^2K_L$ = 4700 mM for sorbose; and f_iT = 65 mmoles/min per cell unit.

is completely general, not requiring the use of a model of transport. Surprisingly, the inward flux of sugar is seen to decay very rapidly with time. Indeed, after 90 sec this influx has vanished, whereas the external concentration has not changed and the internal concentration has dropped by only 25% (from 93 mM to 70 mM). Moreover, curve *a* indicates that the net rate of efflux of sugar has hardly altered during this period.

We might conclude that either the influx of sugar decays rapidly with time or that the assumption of "well-mixing" is here unjustified. The first of these alternatives could be directly tested by performing the procedure of Fig. 8 with the external solution containing only unlabeled glucose for the first 90 sec and only then adding radioactive label. Possible support for this alternative comes from the many instances in which the activity of a catalytic protein has been shown to decay in the presence of substrates or cofactors (Grisolia, 1964). However, it is difficult to understand how this exchange flux could disappear while the net flux remained unaltered. Also, the fact that Miller (1965) has been able to fit reasonably well the countertransport data for the less affine sugars galactose and mannose makes us hesitant to accept this first alternative. However, the second alternative — that the cell interior is not well mixed — is also difficult to accept. This can be seen from a simple calculation. Following Paganelli and Solomon (1957), we consider the cell

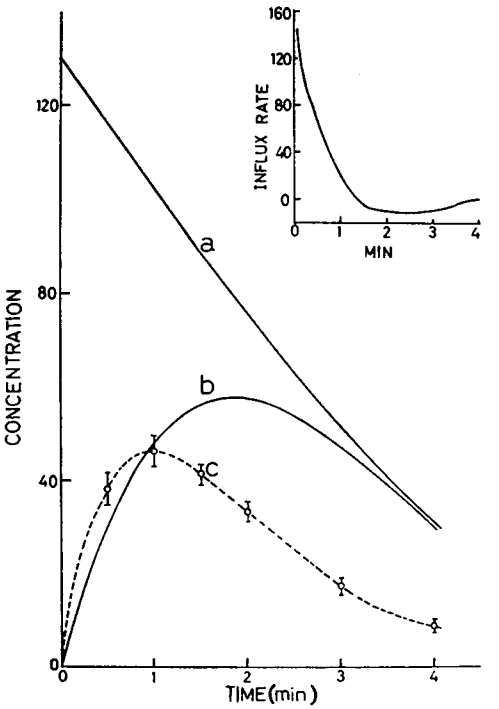

FIGURE 8 Countertransport experiment. Cells previously equilibrated with 130 mM unlabeled glucose were resuspended at zero time in a solution containing labeled glucose at 4.3 mM. The ordinate is the intracellular concentration (mmoles/cell unit) of glucose. Curves *a* and *b* are respectively the intracellular concentrations of total (labeled and unlabeled) and of labeled glucose as predicted by the internal transfer model for K_H = 1.35 mM, K_L = 29 mM, and f_iT = 65 mmoles/min per cell unit. The experimental points are the means (±SD) of the intracellular concentrations of labeled glucose as determined from Table V of Miller (1968 *a*). The dashed line (curve *c*) was drawn by eye through these points. *Insert.* The unidirectional influx of glucose (mmoles/min per cell unit) was calculated from curves *a* and *c* using equation (C 7) of Appendix C, which assumes well-mixing.

as a plane liquid sheet and calculate (using their equation 6) the time required for glucose initially present outside the sheet to reach 90% equilibration inside the cell. It is found that for the cell interior not to be well mixed within 1 sec, the diffusion coefficient for glucose inside the cell would have to be 3000 times less than it is for diffusion in water. This seems most unlikely.

Now, for any model which assumes well-mixing and no decay (and we have seen that these assumptions appear to be reasonable), the cellular concentration of labeled glucose should, as does curve *b*, approach the total cellular concentration (curve *a*) after a few minutes. The fact that the experimental curve *c* does not approach curve *a* presents a real dilemma on any model, and it is perhaps here that further experimental investigations might be useful. In particular, both curves *a* and *c* should be directly obtained from a single experiment.

The second of these procedures (Table III of Miller, 1968 *a*) involves measuring the outflow of radioactive sugar when various unlabeled sugars are present in the external solution at the same concentration (130 mM). For example, when glucose was present on both sides of the membrane the efflux rate was 190 mmoles/min per cell unit; with galactose present on both sides the efflux rate was only 125 mmoles/min per cell unit. This result is not surprising, since it requires only that K_L for galactose be greater than K_L for glucose. What is surprising, however, is that the efflux of glucose into equimolar galactose was 250 mmoles/min per cell unit. Our present, simple model cannot account for this latter finding, but then neither can any previously suggested model. Since this is such an unusual and interesting finding, it would repay further investigation. For instance, if the impermeable mercuric ion in the stopping solution used by Miller (1968 *a*) inhibits only the outward-facing L site of a tetramer, this enhanced glucose-galactose exchange is what the present model would predict. That this is a possibility is suggested by the finding of Kepes (1969) that mercury inhibits asymmetrically the galactoside transport system of *Escherichia coli.*

We have now completed our comparison of the predictions of one type of tetramer model, the internal transfer model, with the experimental data of Miller (1968 *a*). It is apparent that this model accounts for considerably more data than previously published models. It does not account for all the data, however, but those data which it does not accommodate cannot be accounted for by any other presently available model. The present, simple model provides considerable scope for modification, and it will no doubt have to be modified somewhat in the future. Further thought and experimentation might suggest ways in which the model and the data can be brought into accord.

POSSIBLE EXTENSIONS OF THE TETRAMERIC TRANSPORT MODEL TO OTHER SYSTEMS

The success of the tetramer model in its application to the human erythrocyte data has led us to consider its possible relevance to the behavior of other facilitated diffusion systems, including sodium-requiring cotransport systems. An indication of the possible generality of such a model is that many transport systems show a multiplicity of binding sites for substrates, activators, and inhibitors. (A partial listing of such systems is given in Table 8.8 of Stein [1967].) For example, the erythrocyte transport system for glucose itself is inhibited with greater than first-order kinetics by such inhibitors as fluorodinitrobenzene and many analogues of phloretin (Bowyer and Widdas, 1956; LeFevre, 1961). Furthermore, a number of unusual phenomena have recently been reported which can be explained quite naturally on the tetramer model but only with difficulty on the conventional carrier model. One of these is *cis* stimulation, the acceleration of the transport of one substrate by the presence of a second substrate at the same face of the membrane. This has

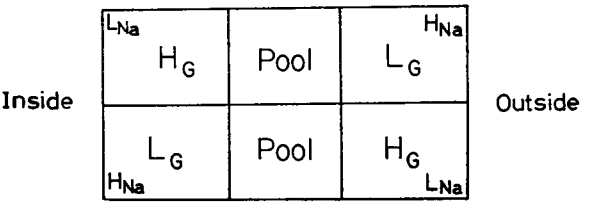

FIGURE 9 Schematic representation of an extension of the internal transport model for a sodium-activated cotransport system. This model is described in detail in the text. The subscripts G and Na refer to substrate and sodium ion, respectively.

been found for amino acid transport in the ascites tumour cell (Jacquez, 1963), in the rabbit ileum (Munck and Schultz, 1969), and in the yeast *Saccharomyces chevalieri* (Magana-Schwencke and J. Schwencke, 1969). Another of these phenomena is *trans* inhibition, the retardation of the transport of one substrate by the presence of a second substrate at the opposite face of the membrane. This has been reported for amino acid transport in ascites tumour cells (Belkhode and Scholefield, 1969; Paine and Heinz, 1960) and for glycine transport in the pigeon erythrocyte (Vidaver and Shepherd, 1968); in this latter paper the *trans* inhibitor is sodium (see below). The complementary phenomena of *cis* inhibition and of *trans* stimulation follow equally naturally from the tetramer or the carrier model.

As an example of how the tetramer model can be extended to other transport systems, we present (Fig. 9) a preliminary model which might apply to some of the sodium-activated cotransport systems involved in the accumulation of amino acids and sugars. The model is completely analogous to that of Fig. 2 for the erythrocyte glucose system, except that the full binding potential of a given subunit is expressed only if a sodium ion is also bound to that subunit. We consider here two possibilities. (*a*) A given subunit has no affinity for substrate in the absence of Na. This rule would predict that the V_{max} but not the K_m for transport would depend upon the concentration of Na. This situation — the V kinetics (Stein, 1967) — has been observed for the cotransport of sugar and sodium ion in the rabbit ileum (Schultz and Zalusky, 1964). (*b*) A given subunit has a low (but finite) affinity for substrate in the absence of Na. This rule would predict the K kinetics, i.e., that the K_m but not the V_{max} for transport would depend upon the concentration of sodium ion. Such behavior has been observed for the cotransport of sugar and sodium ion in the hamster intestine (Crane, 1965). For the particular model of Fig. 9, a subunit having a high affinity for substrate is assumed to have a low affinity for Na and vice versa. For simplicity and symmetry, we again assume the activation rules given in equation 2, where the substrate is the activator.

In order to illustrate the behavior of this model, we will consider two simple situations on the V kinetics. First, let us consider the case when high levels of Na are present on both sides of the membrane. Then each site displays its full binding

potential, and the system behaves exactly as does the erythrocyte glucose system of Fig. 2. In particular, equilibrium exchange of substrate will exhibit an operative K_m of the order of the dissociation constant of the L site. Next, we consider the case when a high level of Na is present at the *cis* face and no Na is present at the *trans* face, and where substrate is present at the *cis* face only. Then only substrate bound at the H subunit will contribute to the flux. Thus, although substrate molecules bound at both H and L sites will enter their respective pools, redistribution of Na ions within the pools by preferential binding to the L subunits allows substrate exit only via the L sites. Thus, substrate initially bound at a *cis* L site will merely return to the *cis* solution and not contribute to the flux. Thus the operative K_m in this situation is that of the high affinity H site. Furthermore, according to the activation rules, the maximal velocity here is one-half that in the equilibrium exchange situation considered above. It is interesting to note that these predictions are approximately borne out by the experiments of Vidaver and Shepherd (1968) on the sodium-glycine cotransport system of the pigeon erythrocyte, although the second-order dependence upon Na found in these experiments might require that two Na ions bind to each subunit. We might note that the differing K_m values operative in the above two situations are sufficient to explain the phenomenon of *trans* inhibition by Na of *cis* to *trans* glycine movement found by Vidaver and Shepherd (1968).

We have considered here only one type of sodium-activated cotransport model. The relevant rules for each transport system will have to be determined individually by appropriate experiments.

EXPERIMENTAL TESTING OF THE TETRAMER MODEL

In order to determine the applicability of the tetramer model to a given transport system, a number of tests may be useful. First, we would expect the paradox of the differing K_m values found by the Sen-Widdas and equilibrium exchange procedures for the human erythrocyte glucose system to manifest itself for other systems. For those systems transporting only a single class of substrate the procedure is obvious from our earlier descriptions. For the cotransport systems involving Na activation, the procedure is similar except that saturating concentrations of Na must be present on both sides of the membrane at all times. Secondly, we would expect that the maximum velocity in an equilibrium exchange experiment be twice that found when substrate is found on one side of the membrane only. This factor of two is expected only if the relevant experiments are performed correctly. By this we mean that all species involved in the transport event, substrate and activator (if relevant), must be present at saturating concentrations on both sides for the former type of experiment but on one side only for the latter type of experiment. Finally, we would expect situations to arise in which K_I for a substrate inhibiting the movement of a second substrate is not identical with either of the operative K_m values obtained when the substrate is studied alone.

We would very much like to thank Professor Aharon Katchalsky for his kind hospitality and to thank him and Professor Ora Kedem for their encouragement and helpful criticism during the course of this work.
We are also grateful to Professor P. G. LeFevre for a critical reading of this manuscript.

We are indebted to the Royal Society and to the Medical Research Council of Great Britain for our personal support (W. D. Stein and W. R. Lieb, respectively).

Received for publication 1 October 1969 and in revised form 9 February 1970.

REFERENCES

BELKHODE, M. L., and P. G. SCHOLEFIELD. 1969. *Biochim. Biophys. Acta.* **173**:290.
BOWYER, F., and W. F. WIDDAS. 1956. *Discuss. Faraday Soc.* **21**:251.
CRANE, R. K. 1965. *Fed. Proc.* **24**:1000.
GRISOLIA, S. 1964. *Physiol. Rev.* **44**:657.
HARRIS, E. J. 1964. *J. Physiol. (London).* **173**:344.
JACQUEZ, J. A. 1963. *Biochim. Biophys. Acta.* **71**:15.
KEPES, A. 1969. *In* The Molecular Basis of Membrane Function. D. C. Tosteson, editor. Prentice-Hall Inc., Englewood Cliffs. 353.
KOSHLAND, D. E., and K. E. NEET. 1968. *Annu. Rev. Biochem.* **37**:359.
LEFEVRE, P. G. 1961. *Pharmacol. Rev.* **13**:39.
LEVINE, M., and W. D. STEIN. 1966. *Biochim. Biophys. Acta.* **127**:179.
MAGANA-SCHWENCKE, N., and J. SCHWENCKE. 1969. *Biochim. Biophys. Acta.* **173**:313.
MARGENAU, H., and G. M. MURPHY. 1943. The Mathematics of Physics and Chemistry. D. Van Nostrand Co., Inc., Princeton. 472.
MILLER, D. M. 1965. *Biophys. J.* **5**:417.
MILLER, D. M. 1968 *a. Biophys. J.* **8**:1329.
MILLER, D. M. 1968 *b. Biophys. J.* **8**:1339.
MONOD, J., J. WYMAN, and J. CHANGEUX. 1965. *J. Mol. Biol.* **12**:88.
MUNCK, B. G., and S. G. SCHULTZ. 1969. *Biochim. Biophys. Acta.* **183**:182.
PAGANELLI, C. V., and A. K. SOLOMON. 1957. *J. Gen. Physiol.* **41**:259.
PAINE, C. M., and E. HEINZ. 1960. *J. Biol. Chem.* **235**:1080.
SCHULTZ, S. G., and R. ZALUSKY. 1964. *J. Gen. Physiol.* **47**:1043.
SEN, A. K., and W. F. WIDDAS. 1962. *J. Physiol. (London).* **160**:392.
STEIN, W. D. 1967. The Movement of Molecules across Cell Membranes. Academic Press, Inc., New York.
STEIN, W. D. 1968. *Nature (London).* **218**:570.
STRYER, L. 1968. *Annu. Rev. Biochem.* **37**:25.
VIDAVER, G. A. 1966. *J. Theor. Biol.* **10**:301.
VIDAVER, G. A., and S. L. SHEPHERD. 1968. *J. Biol. Chem.* **243**:6140.
WILBRANDT, W., and T. ROSENBERG. 1961. *Pharmacol. Rev.* **13**:109.

SYMBOLS AND DEFINITIONS

n	= superscript index which is 1 when referring to sugar species 1, and 2 when referring to sugar species 2. If n is omitted, it is assumed to be 1.
${}^{n}K_{H}$	= dissociation constant (mM) of H binding site for species n.
${}^{n}K_{L}$	= dissociation constant (mM) of L binding site for species n.
${}^{0}K_{H} = {}^{0}K_{L}$	= unity (1) identically, by definition. This is a mathematical symbol with no physical meaning.
${}^{n}M_{c\to t}$	= unidirectional flux (mmoles/min per cell unit) of species n from *cis* to *trans* bathing solutions.
${}^{n}M_{t\to c}$	= unidirectional flux (mmoles/min per cell unit) of species n from *trans* to *cis* bathing solutions.

$^{n}NET_{c\to t}$ = net flux (mmoles/min per cell unit) of species n from *cis* to *trans* bathing solutions.

$^{1+2}NET_{c\to t}$ = total net flux (mmoles/min per cell unit) of both species 1 and 2 from *cis* to *trans* bathing solutions.

$^{n}S_c$ = concentration (mM) of sugar species n in *cis* solution.

$^{n}S_t$ = concentration (mM) of sugar species n in *trans* solution.

$^{0}S_c = {}^{0}S_t$ = unity (1) identically, by definition. This is a mathematical symbol with no physical meaning.

i, j, i', j' = superscript indices or functional arguments which are 0 for no binding of sugar, 1 for binding of species 1, and 2 for binding of species 2.

m, m' = (i or j), (i' or j'), respectively.

$E(i, j; i', j')$ = occupancy state of the tetramer (see Table I) with substrate bound as indicated by the indices at (from left to right) the *cis* H, the *cis* L, the *trans* H, and the *trans* L binding sites.

$[E(i, j; i', j')]$ = concentration (mmoles/cell unit) of the above occupancy state.

$f(i, j; i', j')$ = frequency (min^{-1}) of the transition of the above occupancy state from state A to state B and back to state A.

$^{n}k(i, j; i', j')$ = transfer rate constant of the above occupancy state; i.e., the number of molecules per minute of species n transferred from the *cis* to *trans* bathing solutions by a single tetramer molecule having the above occupancy status.

$^{n}p_H(m; m')$ = probability factor ($0 \leq p \leq 1$), giving the probability that an occupancy state with m bound at the *cis* H site and m' bound at the *trans* L site will transfer a molecule of species n via the channel composing these two sites from the *cis* to *trans* bathing solutions, during a transition of the tetramer from state A to state B and back to state A.

$^{n}p_L(m; m')$ = same as for $^{n}p_H(m; m')$, but substitute *cis* L and *trans* H for *cis* H and *trans* L, respectively.

f_1 = value of $f(i, j; i', j')$ for an occupancy state with only one sugar molecule bound.

T = total concentration (mmoles/cell unit) of tetramer.

cell unit = quantity of cells whose solvent water volume is 1 liter under isotonic conditions.

APPENDIX A

Derivation and Application of Equations for the Unidirectional Fluxes of Two Sugar Species on the Internal Transfer Model

Consider first the *cis* to *trans* flux $^{n}M_{c\to t}$ of species n ($n = 1$ or 2). This will be simply the sum of the contributions from each of the 81 occupancy states, so that

$$^{n}M_{c\to t} = \sum_{i=0}^{2}\sum_{j=0}^{2}\sum_{i'=0}^{2}\sum_{j'=2}^{n} k(i, j; i', j')[E(i, j; i', j')]. \qquad (A\ 1)$$

Since transfer of species n can occur from both the *cis* H and the *cis* L binding sites during

each cycle, the total number of molecules of species n transferred per minute by the occupancy state $E(i, j; i', j')$ is

$$ {}^{n}k(i, j; i', j') = f(i, j; i', j')[{}^{n}p_{H}(i; j') + {}^{n}p_{L}(j; i')] \quad (A\,2) $$

where $f(i, j; i', j')$ is the transition frequency (min^{-1}) of the occupancy state, and the probability factors are as given in Appendix B.

For the case of independent activation via any of the four binding sites,

$$ f(i, j; i', j') = \{4 - \delta_{0,i} - \delta_{0,j} - \delta_{0,i'} - \delta_{0,j'}\}f_1 , \quad (A\,3) $$

where $\delta_{x,y}$ is the Kronecker delta, defined to be unity for $x = y$ and zero for $x \neq y$, and f_1 is a constant characteristic of the tetramer.

By definition, the total concentration of tetramer is just

$$ T = \sum_{i=0}^{2}\sum_{j=0}^{2}\sum_{i'=0}^{2}\sum_{j'=0}^{2}[E(i, j; i', j')]. \quad (A\,4) $$

Because the binding at each site of the tetramer is independent of the binding at any other site and is furthermore an equilibrium situation, then from the definitions of the equilibrium dissociation contants it follows that

$$ [E(i, j; i', j')] = [E(0, 0; 0, 0)]\frac{{}^{i}S_c}{{}^{i}K_H}\frac{{}^{j}S_c}{{}^{j}K_L}\frac{{}^{i'}S_t}{{}^{i'}K_H}\frac{{}^{j'}S_t}{{}^{j'}K_L} . \quad (A\,5) $$

We define a function

$$ D({}^{1}S_c, {}^{1}S_t, {}^{2}S_c, {}^{2}S_t) = \sum_{i=0}^{2}\sum_{j=0}^{2}\sum_{i'=0}^{2}\sum_{j'=0}^{2}\frac{{}^{i}S_c}{{}^{i}K_H}\frac{{}^{j}S_c}{{}^{j}K_L}\frac{{}^{i'}S_t}{{}^{i'}K_H}\frac{{}^{j'}S_t}{{}^{j'}K_L} $$

$$ = \left(1 + \frac{{}^{1}S_c}{{}^{1}K_H} + \frac{{}^{2}S_c}{{}^{2}K_H}\right)\left(1 + \frac{{}^{1}S_t}{{}^{1}K_H} + \frac{{}^{2}S_t}{{}^{2}K_H}\right)\left(1 + \frac{{}^{1}S_c}{{}^{1}K_L} + \frac{{}^{2}S_c}{{}^{2}K_L}\right) $$

$$ \cdot \left(1 + \frac{{}^{1}S_t}{{}^{1}K_L} + \frac{{}^{2}S_t}{{}^{2}K_L}\right). \quad (A\,6) $$

Then, from equations A 4–A 6 it follows that

$$ [E(i, j; i', j')] = \frac{T}{D({}^{1}S_c, {}^{1}S_t, {}^{2}S_c, {}^{2}S_t)}\frac{{}^{i}S_c}{{}^{i}K_H}\frac{{}^{j}S_c}{{}^{j}K_L}\frac{{}^{i'}S_t}{{}^{i'}K_H}\frac{{}^{j'}S_t}{{}^{j'}K_L} . \quad (A\,7) $$

Thus, we finally arrive at a complete analytical solution for the fluxes

$$ {}^{n}M_{c\to t} = \sum_{i=0}^{2}\sum_{j=0}^{2}\sum_{i'=0}^{2}\sum_{j'=0}^{2}f(i, j; i', j')\{{}^{n}p_{H}(i; j') + {}^{n}p_{L}(j; i')\} \quad (A\,8) $$

$$ \cdot [E(i, j; i', j')], $$

where

$$ (i, j; i', j') = \{4 - (\delta_{0,i} + \delta_{0,j} + \delta_{0,i'} + \delta_{0,j'})\}f_1 $$

$$ {}^{n}p_{H}(i; j') = \frac{\delta_{i,n}}{1 + \left[\left(\frac{{}^{1}K_{H}}{{}^{1}K_{L}}\right)^{(j'+n-2)} \left(\frac{{}^{2}K_{L}}{{}^{2}K_{H}}\right)^{\frac{(j'+n-1)}{2}}\right]^{(n-j')}} $$

$$ {}^{n}p_{L}(j; i') = \frac{\delta_{j,n}}{1 + \left[\left(\frac{{}^{1}K_{L}}{{}^{1}K_{H}}\right)^{(i'+n-2)} \left(\frac{{}^{2}K_{H}}{{}^{2}K_{L}}\right)^{\frac{(i'+n-1)}{2}}\right]^{(n-i')}} $$

$$ [E(i, j; i', j')] = \frac{T}{D({}^{1}S_{c}, {}^{1}S_{t}, {}^{2}S_{c}, {}^{2}S_{t})} \frac{{}^{i}S_{c}}{{}^{i}K_{H}} \frac{{}^{j}S_{c}}{{}^{j}K_{L}} \frac{{}^{i'}S_{t}}{{}^{i'}K_{H}} \frac{{}^{j'}S_{t}}{{}^{j'}K_{L}} $$

$$ D({}^{1}S_{c}, {}^{1}S_{t}, {}^{2}S_{c}, {}^{2}S_{t}) $$

$$ = \left(1 + \frac{{}^{1}S_{c}}{{}^{1}K_{H}} + \frac{{}^{2}S_{c}}{{}^{2}K_{H}}\right)\left(1 + \frac{{}^{1}S_{t}}{{}^{1}K_{H}} + \frac{{}^{2}S_{t}}{{}^{2}K_{H}}\right)\left(1 + \frac{{}^{1}S_{c}}{{}^{1}K_{L}} + \frac{{}^{2}S_{c}}{{}^{2}K_{L}}\right)\left(1 + \frac{{}^{1}S_{t}}{{}^{1}K_{L}} + \frac{{}^{2}S_{t}}{{}^{2}K_{L}}\right) $$

and

$$ {}^{0}S_{c} = {}^{0}S_{t} = {}^{0}K_{H} = {}^{0}K_{L} = 1. $$

Because the system is symmetric, the *trans* to *cis* fluxes ${}^{n}M_{t\to c}$ ($n = 1$ or 2) can be obtained by interchanging the *cis* and *trans* solutions, i.e. by simply interchanging the subscripts (c) and (t) in (A 8). Notice that only the term $[E(i, j; i', j')]$ is altered by this interchange, the other terms in (A 8) being invariant to such an operation. Furthermore the factor $D({}^{1}S_{c}, {}^{1}S_{t}, {}^{2}S_{c}, {}^{2}S_{t})$ of $[E(i, j; i', j')]$ is also invariant to this interchange. The above equations may look complicated, but they involve only elementary arithmetic operations (no calculus) and can therefore be easily manipulated, especially with a computer.

In obtaining the values of the concentrations $({}^{1}S_{c}, {}^{1}S_{t}, {}^{2}S_{c}, {}^{2}S_{t})$ for use in the flux equations, one must be careful to correct for cell volume changes. This can easily be done (Miller, 1968 *b*) by dividing the cellular concentration of sugar given in terms of cell units (liters of isotonic cell water) by a factor which is the ratio of the total intracellular osmolarity per cell unit to the external osmolarity per liter of solution. The detailed procedure for the case of sugar transport in the human erythrocyte is given by Miller (1968 *b*).

We now demonstrate how the undetermined constants of (A 8) can be determined from the experimental data. First we consider the data involving experiments with only one sugar — glucose. For these there are three undetermined constants: ${}^{1}K_{H}$, ${}^{1}K_{L}$, and $f_{i}T$. The latter constant, $f_{i}T$, is simply obtained from the maximum velocity V_{max} of the equilibrium exchange procedure. The maximum velocity is reached when all four tetramer binding sites are complexed with glucose molecules. In this situation equation A 8 reduces to

$$ {}^{1}M_{c\to t} = {}^{1}M_{t\to c} = f(1, 1; 1, 1)[E(1, 1; 1, 1)] = 4f_{i}T = V_{max}. \qquad (A\ 9) $$

Since in this situation V_{max} = 260 mmoles/min per cell unit (Miller, 1968 *b*), $f_{i}T$ = 65 mmoles/min per cell unit. The second constant, ${}^{1}K_{L}$, is also simply obtained from the equilibrium exchange experiment data. It is found that for the case when ${}^{1}K_{L} \gg {}^{1}K_{H}$, as is the case at 20°C for the human erythrocyte glucose system, the predictions of the internal transfer model for this experiment are relatively insensitive to the exact value of ${}^{1}K_{H}$. By assigning a reasonable value of ${}^{1}K_{H}$ = 2 mM and knowing $f_{i}T$ = 65 mmoles/min per cell unit, it was found that the value of ${}^{1}K_{L}$ = 29 mM best fits the experimental data from Table IV of Miller

(1968 *a*). (The criterion for best fit was that the algebraic sum of deviations was a minimum.) Finally, having obtained the best values for f_1T and ${}^1K_L$, the best value of ${}^1K_H$ was determined using the data from the Sen-Widdas experiment. It was found that the value of ${}^1K_H = 1.35$ mM best fits the experimental data from Table I of Miller (1968 *a*). To summarize, with the convention that species 1 is glucose, the values ${}^1K_H = 1.35$ mM, ${}^1K_L = 29$ mM, and $f_1T = 65$ mmoles/min per cell unit best fit the relevant experimental data of Miller (1968 *a*). These values were used for all of the predictions of the internal transfer model given in this paper.

In order to calculate the model predictions for the experiments in which the movement of sorbose was inhibited by glucose, estimates of ${}^2K_H$ and ${}^2K_L$ were required in addition to the above parameters. Unfortunately, experimental data for sorbose using the equilibrium exchange and Sen-Widdas procedures are not available, so a unique pair of values could not be obtained. However, the values ${}^2K_H = 1500$ mM and ${}^2K_L = 4700$ mM gave a good fit to the data (see Fig. 7).

Finally, the model predictions for the countertransport experiment (curves *a* and *b* of Fig. 8) were calculated by numerical integration on a digital computer, using the Runge-Kutta method (Margenau and Murphy, 1943) with a time increment of 0.001 min. Since only glucose (both labeled and unlabeled) is involved here, no new parameters had to be determined. The calculation of the curve given in the insert to Fig. 8 was performed as described in Appendix C.

APPENDIX B

Derivation of Internal Transfer Probabilities

Although the internal transfer probabilities can be derived in a straightforward manner from the model of Fig. 2 through the minimization of the total free energy of binding in a given channel of the system in state B (see Fig. 3), more insight into the constraints afforded by the transport process itself can be obtained by the more general derivation which follows. Advantages of the present treatment are that it requires few assumptions as to transfer mechanism and it can easily be modified to take care of other activation rules.

Recall that in the internal transfer model the binding of substrate at one binding site has no effect upon binding at any of the other three sites; the only effect of such binding is to increase the frequency of a transition between states A and B, and this is also done independently of any binding at the other sites. This lack of obligatory coupling between the binding sites is important in the following analysis.

We perform the following gedankenexperiment. In principal, there is no reason to suppose that reagents cannot be found which can (*a*) specifically inhibit binding at either an H or an L site with no other effect and (*b*) act on the binding sites at only one face of the membrane in a given experiment. In this manner it would be possible to so inhibit the tetramer of Fig. 2 that the bottom channel were functionally inoperative, leaving only the upper channel operative as a complete transport system. We can then apply the second law of thermodynamics to this subsystem, thus obtaining the desired rules. Because of our assumption of independence and nonobligatory coupling between the binding sites and hence the channels, the rules so obtained will also apply to the uninhibited transport system.

To be specific, we adopt the nomenclature defined in the Symbols and Definitions. With reference to Fig. 2, we call the inside solution (bathing the H subunit of the upper channel) the *cis* solution. We consider the situation where the *cis* and *trans* solutions have identical chemical compositions, so that

$$ {}^1S_c = {}^1S_t = {}^1S \quad \text{and} \quad {}^2S_c = {}^2S_t = {}^2S. \tag{B 1} $$

In this situation the second law of thermodynamics requires that the operation of the isolated upper channel be such that no gradients of either sugar 1 or sugar 2 become established between the two bathing solutions. But this requires the equality of the two unidirectional fluxes for each sugar, or

$$ {}^1M_{c\to t} = {}^1M_{t\to c} \quad \text{and} \quad {}^2M_{c\to t} = {}^2M_{t\to c}\,. \tag{B 2} $$

Application of equation A 8 and its symmetrical analogue to this situation, allowing for the strict absence of possible binding at the L and H sites in the lower channel of Fig. 2, leads to the following two expressions:

$$ {}^1M_{c\to t} = \frac{f_1 T\,{}^1S}{{}^1K_H D'({}^1S, {}^2S)}\left[{}^1p_H(1;0) + \frac{2\,{}^1S}{{}^1K_L}\,{}^1p_H(1;1) + \frac{2\,{}^2S}{{}^2K_L}\,{}^1p_H(1;2)\right] \tag{B 3} $$

$$ {}^1M_{t\to c} = \frac{f_1 T\,{}^1S}{{}^1K_L D'({}^1S, {}^2S)}\left[{}^1p_L(1;0) + \frac{2\,{}^1S}{{}^1K_H}\,{}^1p_L(1;1) + \frac{2\,{}^2S}{{}^2K_H}\,{}^1p_L(1;2)\right] \tag{B 4} $$

where

$$ D'({}^1S, {}^2S) = \sum_{i=0}^{2}\sum_{j'=0}^{2} \frac{{}^iS}{{}^iK_H}\,\frac{{}^{j'}S}{{}^{j'}K_L}, \quad \text{with} \quad {}^0S \equiv 1. $$

The corresponding expressions for the fluxes of species 2 are obtained simply by interchanging 1 and 2 in the above expressions wherever they appear as indices, i.e. either as superscripts or as functional arguments.

Equating equation B 3 with equation B 4, and then cancelling common terms, gives

$$ {}^1K_L\,{}^1p_H(1;0) + 2\,{}^1p_H(1;1)\,{}^1S + \frac{2\,{}^1K_L}{{}^2K_L}\,{}^1p_H(1;2)\,{}^2S = {}^1K_H\,{}^1p_L(1;0) + 2\,{}^1p_L(1;1)\,{}^1S + \frac{2^1K_H}{{}^2K_H}\,{}^1p_L(1;2)\,{}^2S. \tag{B 5} $$

Because the variables ${}^1S$ and ${}^2S$ are independent of each other, and equation B 5 must be valid for all values of these two independent variables, the constant terms and the coefficients of corresponding terms in ${}^1S$ and ${}^2S$ on each side of the equality must respectively equal each other. Thus

$$ {}^1K_L{}^1p_H(1;0) = {}^1K_H{}^1p_L(1;0) \tag{B 6} $$

$$ {}^1p_H(1;1) = {}^1p_L(1;1) \tag{B 7} $$

$$ \frac{{}^1K_L}{{}^2K_L}\,{}^1p_H(1;2) = \frac{{}^1K_H}{{}^2K_H}\,{}^1p_L(1;2), \tag{B 8} $$

with similar expressions obtained by interchanging indices 1 and 2.

The remaining equations necessary for an exact solution for the probability factors are obtained directly from the condition that any sugar molecule within the pool in the B state of the tetramer must leave the pool during the B to A conformation change. Thus,

$$ {}^1p_H(1;0) + {}^1p_L(1;0) = 1 \tag{B 9} $$

$$^1p_H(1;1) + {}^1p_L(1;1) = 1 \tag{B 10}$$

$$^1p_H(1;2) + {}^1p_L(1;2) = 1, \tag{B 11}$$

with similar expressions obtained by interchanging indices 1 and 2.

Solving equations B 6–B 11 yields

$$^1p_H(1;0) = \frac{^1K_H}{^1K_H + {}^1K_L} \tag{B 12}$$

$$^1p_L(1;0) = \frac{^1K_L}{^1K_H + {}^1K_L} \tag{B 13}$$

$$^1p_H(1;1) = {}^1p_L(1;1) = 0.5 \tag{B 14}$$

$$^1p_H(1;2) = \frac{^1K_H\,{}^2K_L}{^1K_H\,{}^2K_L + {}^1K_L\,{}^2K_H} \tag{B 15}$$

$$^1p_L(1;2) = \frac{^1K_L\,{}^2K_H}{^1K_H\,{}^2K_L + {}^1K_L\,{}^2K_H}, \tag{B 16}$$

with the corresponding six probability factors for species 2 obtained by interchanging indices 1 and 2.

Finally, by definition, the remaining 24 probability factors (each referring to the *cis* to *trans* movement of a sugar molecule not initially bound at the *cis* face of a given channel) are identically zero.

For ease of computation, especially with a computer, these 36 probability factors can be simply expressed by the following two equations:

$$^np_H(i;j') = \frac{\delta_{i,n}}{1 + \left[\left(\frac{^1K_H}{^1K_L}\right)^{(j'+n-2)}\left(\frac{^2K_L}{^2K_H}\right)^{\left(\frac{j'+n-1}{2}\right)}\right]^{(n-j')}} \tag{B 17}$$

$$^np_L(j;i') = \frac{\delta_{j,n}}{1 + \left[\left(\frac{^1K_L}{^1K_H}\right)^{(i'+n-2)}\left(\frac{^2K_H}{^2K_L}\right)^{\left(\frac{i'+n-1}{2}\right)}\right]^{(n-i')}}, \tag{B 18}$$

where the index n may be either 1 or 2, the indices i, j, i', j' may be 0, 1, or 2, and $\delta_{x,y}$ is the Kronecker delta function, defined to be unity for $x = y$ and zero for $x \neq y$.

Notice that the probability factors do not depend upon the absolute values of the H and L site dissociation constants for a given sugar, but only upon their ratio.

APPENDIX C

Calculation of Decay of Influx during Countertransport Assuming a Well-Mixed Interior Compartment

We refer to a countertransport situation such as performed by Miller (1968 *a*) and described under Fig. 8. Unlabeled and labeled glucose are denoted by indices 1 and 2, respectively. The cytoplasm is considered to be the *cis* solution. The external, *trans*, solution is composed

of labeled glucose and is so much larger in volume than the *cis* solution that its composition may be assumed to remain constant with time.

At any time the net efflux of total sugar from the cell is

$$^{1+2}\mathrm{NET}_{c\to t} = {}^{1}\mathrm{NET}_{c\to t} + {}^{2}\mathrm{NET}_{c\to t}\,. \qquad (C\,1)$$

However, since the *trans* solution contains only labeled sugar,

$$^{1}\mathrm{NET}_{c\to t} = {}^{1}M_{c\to t} \qquad (C\,2)$$

$$^{2}\mathrm{NET}_{c\to t} = {}^{2}M_{c\to t} - {}^{2}M_{t\to c}\,. \qquad (C\,3)$$

From equations C 1–C 3 we obtain the desired unidirectional influx at any time as

$$^{2}M_{t\to c} = {}^{1}M_{c\to t} + {}^{2}M_{c\to t} - {}^{1+2}\mathrm{NET}_{c\to t}\,. \qquad (C\,4)$$

The assumption of instantaneous cellular mixing requires that

$$\frac{^{2}M_{c\to t}}{^{1}M_{c\to t}} = \frac{^{2}S_c}{^{1}S_c}. \qquad (C\,5)$$

Substituting equation C 5 into equation C 4 and rearranging yields

$$^{2}M_{t\to c} = \left[1 + \frac{^{2}S_c}{^{1}S_c}\right] {}^{1}M_{c\to t} - {}^{1+2}\mathrm{NET}_{c\to t}\,. \qquad (C\,6)$$

Finally, substituting equations C 1 and C 2 into equation C 6 and rearranging yields the desired result:

$$^{2}M_{t\to c} = \frac{^{2}S_c}{^{1}S_c}\,{}^{1+2}\mathrm{NET}_{c\to t} - \left[1 + \frac{^{2}S_c}{^{1}S_c}\right] {}^{2}\mathrm{NET}_{c\to t}. \qquad (C\,7)$$

The curve of the influx $^{2}M_{t\to c}$ vs. time, plotted in the insert to Fig. 8, was calculated from equation C 7 as follows. The values of the ratio $^{2}S_c$:$^{1}S_c$ were calculated from the ratio of the values given by (*a*) curve *c* and (*b*) the difference between curves *a* and *c* of Fig. 8. The net efflux rates $^{1+2}\mathrm{NET}_{c\to t}$ and $^{2}\mathrm{NET}_{c\to t}$ were calculated from the slopes of curves *a* and *c*, respectively. The slopes were calculated at intervals of 0.05 min using a digital computer.